Date of publication SEP-30, 2025, date of current version AUG-19, 2025.
www.computingonline.net / computing@computingonline.net

Print ISSN 1727-6209
Online ISSN 2312-5381
DOI 10.47839/ijc.24.3.4192

Information Technologies for Digital Control of Transporters of Book Blocks Conveyor Dryers Drive

BOHDANA FEDYNA, OLGA FEDEVYCH, YURII LYSYI, NATALIIA LYSA, LIUBOMYR SIKORA
Lviv Polytechnic National University, Lviv, 79013 Ukraine

Corresponding author: Olga Fedevych (e-mail: olha.y.fedevych@lpnu.ua).

ABSTRACT This article explores information technologies for the digital control of conveyor dryer transporter drives used in the drying of book blocks. The article analyzes the requirements for automated control systems for electric drives, particularly variable-frequency induction motors used in printing production lines. A digital control system architecture is proposed, ensuring flexible adjustment of operating modes, energy consumption optimization, and increased reliability of drying installations. The study describes advanced control algorithms for regulating the speed and torque of the electric drive using modern microcontrollers and sensor technologies. These solutions enable real-time adaptive adjustments to technological conditions, thereby improving overall system efficiency. Particular attention is paid to the integration of predictive maintenance functions and fault detection mechanisms, which enhance system reliability and reduce downtime. Experimental studies confirm the effectiveness of the developed approach, demonstrating improved performance and energy efficiency. The proposed solutions can be applied to modernize automated control systems in the printing industry, contributing to increased productivity, higher drying quality, and lower operational costs.

KEYWORDS asynchronous motor; printing products; pulse speed sensor; lattice functions; structure; digital structural modeling; drying quality; thermodynamic interaction.

I. INTRODUCTION AND PROBLEM STATEMENT

To optimize the drying processes of printed products, it is necessary to develop and implement two interrelated control systems: the temperature of the medium and the movement of these products in the drying chambers.

In modern dryers, the spines of book blocks and other products are dried at an approximately constant temperature and the speed of the continuous movement of conveyors carrying the products to be dried. The temperature in the dryers and the speed of the conveyors is set by the operator based on their own experience, using outdated technical equipment with limited capabilities. Other possible drying modes—particularly those involving precise pauses of bundled printed materials under or between lamp sources of infrared radiation and with the corresponding intensity of heat energy change [9, 20, 25] have not been studied and are not used. To determine and implement rational modes of drying printing products in different dryers with different types of dehydrated products and methods of their placement on conveyors, it is advisable to use computers and digital methods and means of coordinated regulation of the thermal energy sources and conveyor movement. Relatively cheap thyristor converters (TC) are also needed to change the supply voltage of the lamps and the frequency of the supply current to the induction motors of the conveyors. To achieve this, it is sufficient to implement only the temperature and speed control functions of only the temperature and speed controllers and conveyor movement controllers in software, and to use these software tools for control instead of analog controllers in typical TCs. Since it is sufficient to change the voltage and current frequency within the range of (5÷10):1, and it is permissible to regulate the speed of the conveyor motor according to the law U/f = const, the use of expensive frequency converters (FC), in particular, from foreign manufacturers (such as ALTIVAR, MRS-310, etc.), which are equipped with dedicated computer units running complex software, is impractical for dryers.

We previously developed a temperature control system for book block dryers, as described in [8]. This article proposes algorithms and programs for digital setpoints and controllers of the conveyor induction motor speed and displacement and formulas for engineering calculations of their parameters, along with mathematical models and simulation programs for analyzing the dynamic properties of the drives based on the FC-AM (asynchronous motor) system.

II. ANALYSIS OF THE RESULTS OF PREVIOUS STUDIES AND PUBLICATIONS DEVOTED TO SOLVING THE PROBLEM

Typical drying processes for printed products are described in [9, 10, 12], though the methods and modern tools for their optimization are not addressed. In [9], the concept of drying book blocks using intermittent conveyor movement and variable lamp power is merely introduced. In [3, 5, 18, 19] and many other literary sources, methods of digital control of frequency converters, including vector control, which enable wide-range regulation of AM rotational speed under various control strategies. Paper [2] describes the TPTR-6.3-400-200/50 type FC with analog PPCS (pulse-phase control system) and digital power, torque, and speed controllers. Mass production of digitally controlled frequency converters has not yet been established in Ukraine.

For conveyor systems in printing dryers, it is advisable to implement programmatic control of the frequency converter and lamp power supply using a single computer. In addition, the computer should control fans, dampers, and valves, as well as be used for metering, protection, and signaling functions. The same computer can collect statistical data to support the identification of rational drying modes for printed products.

These works explore the method of laser sensing of paper sheets using a variable-power photon beam, as substantiated in [11, 13-17, 21-23].

III. MATHEMATICAL MODELS AND ENGINEERING METHODS FOR SELECTING CONTROL MEANS OF DRIVES BASED ON THE FC-AM SYSTEM

The most advanced and widely used drives are thyristor-based DC and AC systems with subordinate control mechanisms of such coordinates as voltage, currents, magnetic flux, rotational speed, motor torque, and movement of working bodies of mechanisms [5, 6, 24].

For drives, in particular, DC drives with analog linear and linearized components, structural diagrams, and formulas for selecting controller types and calculating their parameters that optimize circuits and provide stability, permissible overshoot within 5–8%, and a control error of ±2–5%, which is acceptable for most production mechanisms, and speed are theoretically substantiated. Optimization methods for control systems of asynchronous drives with frequency converters involve more complex algorithms, schemes, software, and hardware than those for DC drives [3, 5]. For dryer conveyor drives, the simplified control schemes and software for digital FCs described below are considered acceptable.

IV. DEVELOPMENT OF A DIGITAL CONTROL SYSTEM FOR A VARIABLE FREQUENCY DRIVE

The linearized mechanical frequency characteristics of drives based on the FC-AM system are presented in Fig. 1. Their operational segments can be assumed to be equidistant. The natural mechanical characteristic (at the frequency $f_{ном}$ and the supply voltage of the stator phase winding $U_{ном}$) is depicted with linearized working and start-brake segments and is taken as the basis for calculating the parameters of the ATS. The characteristics shown in Fig. 1 are inherent in the drives when f and U_f change according to the law f/U_f = const, which is suitable for regulating conveyor speed. That is, $f / f_n = U_f / U_{fn} = \alpha$.

In this case, the torque of the asynchronous motor (AM) is calculated using the following formula:

$$M = \frac{3 U_{f\,n}^2 \cdot R_2}{\omega_{0\,f_н} \cdot \alpha \cdot s_{AM}\,[(R_1/\alpha + R_2/(\alpha \cdot s_{AM}))^2 + (x_1 + x_2)^2]}, nm \quad (1)$$

where $\omega_{0\,f_н}$ is the stator magnetic field rotation frequency in rad/s at $f = f_n$; s_{AM} is the rotor slip:

$$s_{AM} = (\omega_{0\,f_н} \cdot \alpha - \omega)/(\omega_{0\,f_н} \cdot \alpha) = 1 - \omega/(\omega_{0\,f_н} \cdot \alpha), \quad (2)$$

where R_1, R_2, x_1 and x_2 are the active and inductive resistances of the stator and rotor phase windings reduced to the stator winding. A more accurate torque calculation formula also exists, accounting for winding leakage and mutual induction [4].

Taking into account the accepted parallelism of the working parts of the mechanical characteristics of the AM, in the absence of the ω controller, the rotational speed on each segment is given by:

$$\omega_f = \omega_{0f} - \frac{M}{M_н}\Delta\omega_н = \omega_{0f} - \Delta\omega, \quad (3)$$

where M_n and M are the nominal and operating torque values; ω_{0f} and ω_f is the rotational speed of the magnetic field and rotor at frequency f; $\Delta\omega_н = \omega_{0f_н} - \omega_н$; ω_n is the nominal rotational speed at f_n and M_n.

In the presence of the regulator ω, the FC changes the frequency f (in Fig. 1 $f > f_n$). At the same time, the regulator decreases $\Delta\omega$. The regulator ω can act according to the PI and P-law. A block diagram of the drive with an inertial encoder 3d and a regulator ω is shown in Fig. 2. In the scheme, the FC generates α (in reality, U_f, equal to $\alpha \cdot U_{fn}$ and f, equal to $\alpha \cdot fn$). The transmission coefficient kα is determined by the expression: $k\alpha = \alpha_{ном}/U_{reg\ ном}$.

If $U_{reg\ ном}$=10 V, then $\alpha_{ном}$=1, i.e. k_α=0.1. The scheme in Fig. 2 provides for the use of a more accurate PI controller ω. The transfer coefficient of the controller ω $k_{p\,\omega}$ and the feedback coefficient of ω $k_{з\,\omega}$ are to be determined. The transmission coefficient of the encoder k_z is assumed to be 1. It is also necessary to determine the time constants of 3d and the PI-controller ω. The time constant of the FC inertia is relatively small (T_{FC} = 0.001 ÷ 0.005 s). The electromagnetic inertia of the AM is insignificant compared to the mechanical time constant T_M and is not taken into account.

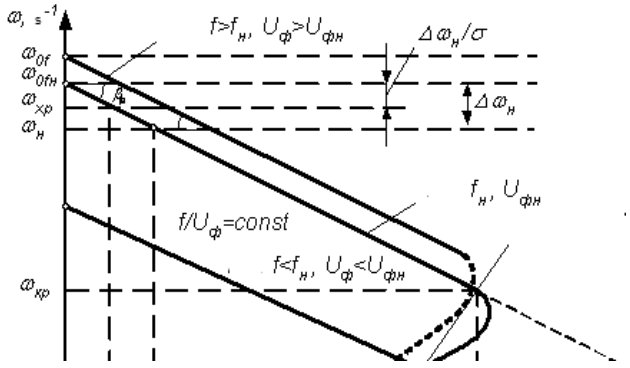

Figure 1. Frequency mechanical characteristics of the drive by the FC-AM system

According to the structural diagram (Fig. 2), in static, the magnetic field rotation frequency $\omega_{0\,f}$ at a current frequency f is equal to $\omega_{0\,f} = \omega_{0\,f_н} \cdot \alpha$, where

$\alpha = k_{p\omega} \cdot k_\alpha \cdot (U_з - k_{з\omega} \cdot \omega_f)$.

When M = Mн

$$\omega_f = \omega_{0\,f} - \Delta\omega_н = k_{p\omega} \cdot k_\alpha (U_з - k_{з\omega} \cdot \omega_f)\omega_{0\,f_н} - \Delta\omega_н. \quad (4)$$

That is $\omega_f = \dfrac{k_{p\omega} \cdot k_\alpha \cdot U_з \cdot \omega_{0\,f_н}}{\sigma} - \dfrac{\Delta\omega_н}{\sigma}$,

where $\sigma = 1 + k_{p\omega} \cdot k_\alpha \cdot k_{з\omega} \cdot \omega_{0f_н}$.

At $U_з = U_{зн} = 10\,V$.

Therefore $k_{p\omega} \cdot 0{,}1 \cdot 10/\sigma = 1$, and $k_{p\omega} = \sigma$.

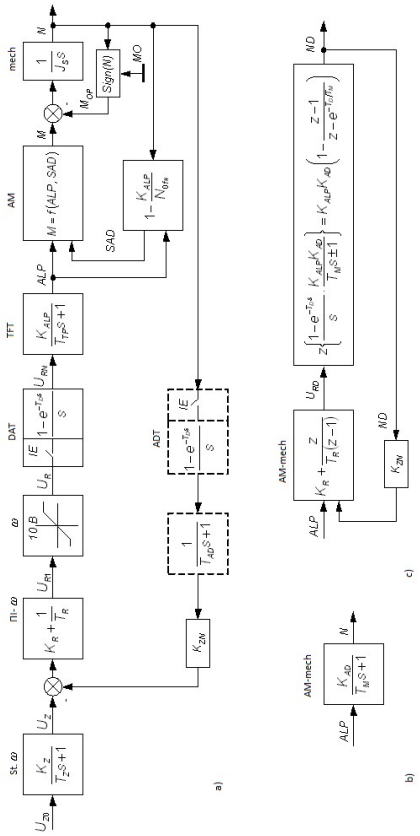

Figure 2. Structural diagram of the drive by the FC-AM system

That is, to reduce $\Delta\omega_н$ by a factor of 10, for example, from 6 to 0.6 % of $\omega_{0\,f_н}$, it is necessary that $k_{p\omega} = 10\,V/V$. At the same time, the feedback coefficient on ω will be equal to :

$$k_{з\omega} = (\sigma - 1)/(k_{p\omega} \cdot k_\alpha \cdot \omega_{0\,f_н}) = (10 - 1)/(10 \cdot 0{,}1 \cdot \omega_{0\,f_н}) = 9/\omega_{0\,f_н}. \quad (5)$$

We can take $k_{з\omega} = 10/\omega_{0\,f_н}$, which is equivalent to $k_{з\omega} = U_{зн}/\omega_{f_н}$.

To optimize the dynamic properties of an induction drive according to the modular optimum (Betrags optimum [5, 6]), a PI controller ω is acceptable. In this case, the FC inertia is not compensated. In the structural diagram of the drive, the AM and the mechanism can be represented in the form with the transfer function $W_{AM-мех}(s) = k_{AM}/(T_M s \pm 1)$, where $k_{AM} = \omega_{f_н}/\alpha_{ном}$, and T_M is the mechanical time constant proportional to the total moment of inertia of the drive J_Σ, and different in value when the drive moves on the operating and starting-braking parts of the mechanical characteristics of the AM. The motion of the actuator at $\omega < \omega_{кр}$ (Fig. 1) is described by Eq:

$$J_\Sigma \frac{d\omega}{dt} = M_n + \frac{M_{кр} - M_n}{\omega_{кр}} \cdot \omega - M_{on},$$

$$\text{or} \quad J_\Sigma \frac{\omega_{кр}}{M_{кр} - M_n} \cdot \frac{d\omega}{dt} - \omega = \frac{(M_n - M_{on}) \cdot \omega_{кр}}{M_{кр} - M_n}, \quad (6)$$

where M_n, M_{kp} and M_{on} are the starting, critical and resistance moments; Mon is assumed to be constant and not greater than M_n; M_n and M_{kp} have different values at different values of f and U_f.

In symbolic form (at s = d/dt), the equation of motion is as follows:

$$(T_M s - 1) \cdot \omega(t) = (M_n - M_{on}) \cdot \omega_{кр}/(M_{кр} - M_{on}), \quad (7)$$

where Tm = JΣ -ω_{kp} / (M_{kp} - M_{on}).

The equation of motion at $\omega > \omega_{kp}$ is as follows:

$$J_\Sigma \frac{d\omega}{dt} = M_\partial - M_{on}, \quad (8)$$

where M_∂ can be expressed as a function of ω in the forms:

$$M_\partial = M_н - \frac{M_н(\omega - \omega_н)}{\omega_0 - \omega_н} = M_н\left(1 - \frac{\omega - \omega_н}{\omega_0 - \omega_н}\right) = \frac{M_н(\omega_0 - \omega)}{\omega_0 - \omega_н};$$

$$M_\partial = M_{кр} - \frac{M_{кр}(\omega - \omega_{кр})}{\omega_0 - \omega_{кр}} \text{ and } M_\partial = M_{к.з.ф} - \frac{M_{к.з.ф}}{\omega_0} \cdot \omega,$$

where $M_{к.з.ф}$ is the dummy torque at $\omega = 0$ (Fig. 1).

After accepting $M_\partial = M_н(\omega_0 - \omega)/(\omega_0 - \omega_н)$, we get

$$J_\Sigma \frac{\omega_0 - \omega_н}{M_н} \frac{d\omega}{dt} + \omega = \omega_0 - \frac{M_{on}}{M_н}(\omega_0 - \omega_н),$$

$$\text{or} \quad (T_M s + 1)\omega = \omega_0 - \frac{M_{on}}{M_н}(\omega_0 - \omega_н), \quad (9)$$

where $T_M = J_\partial(\omega_0 - \omega_н)/M_н$.

The optimization of the automatic adjustment system (AAS) contours compensates for the effects of time constants of the most inertial elements. In the FC-AM system, such a time constant is T_M. At least one integrating link is required for astatic control in the optimized AAS.

The transfer function of the drive according to the FC-AM system with a PI controller ω and an open feedback loop according to ω (Fig. 2) is as follows:

$$W^p_{FC-AM}(s) = \frac{k_\alpha \cdot k_{AM}(T_{R2} s + 1)}{(T_{TP} \cdot T_{R1} s^2 + T_{R1} s)(T_M s + 1)}, \quad (10)$$

where T_{R1} and T_{R2} are the time constants of the PI controller; $T_{R2} = k_R \cdot T_{R1}$; is the time constant of the FC.

At $T_{R2} = T_M$, the transfer function of the closed-loop drive system is as follows:

$$W^з_{FC-AM}(s) = \frac{W^p_{FC-AM}(s)}{1 + k_{з\omega} \cdot W^p_{FC-AM}(s)} = \frac{1/k_{з\omega}}{T_{TP} \cdot T_{R1\,екв} \cdot s^2 + T_{R1\,екв} \cdot s + 1}, \quad (11)$$

where $T_{R1\,екв}$ is the equivalent integration constant of the controller

$$T_{R1\,екв} = T_{R1}/k_{AM} \cdot k_\alpha \cdot k_{з\omega}. \quad (12)$$

The transient process with 4.3 % overshoot and with a time of 4.7 T_μ to the first steady-state value of the regulated parameter is provided in systems if their transfer function is as follows [6]:

$$W(s) = \frac{1}{2T_\mu^2 s^2 + 2T_\mu s + 1}, \quad (13)$$

where T_μ is the uncompensated time constant ($T\mu = 0{,}004 \div 0{,}01\ s$).

Since the relative damping coefficient ξ is equal to $\xi = T_{R1\,екв}/(2\sqrt{T_{TP} \cdot T_{R1\,екв}})$, it is necessary that $T_{R1\,екв} = 2T_\mu$ and $T_{TP} \cong T_\mu$. Then $\xi = 1/\sqrt{2}$. The time constant of the FC is close to T_μ. Therefore, the parameters of the PI controller ω can be determined by the expressions:

$$T_{R1} = 2T_{TP} \cdot k_\alpha \cdot k_{AM} \cdot k_{з\omega};\ T_{R2} = T_M;\ k_R = T_{R2}/T_{R1}.$$

Given the small value of T_{TP}, the optimized transfer function of the drive can be taken in the form

$$W^{onm}_{FC-AM}(s) = \frac{1/k_{з\omega}}{2T_{TP}s + 1} \qquad (14)$$

When $\omega > \omega_{кр}$ the AM mechanism is described by the transfer function of the aperiodic link, and in transients with $\omega < \omega_{кр}$ the function $W_{AD-M}(s) = k_{AD}/(T_M s - 1)$. The intensity of acceleration of the AM without boosting is large, and it can be reduced by an inertial setpoint with $T_{з\partial} \le T_M$.

If it is necessary to regulate the path of the conveyor (in the intermittent mode of its movement), the PI controller ω can perform the function of a PI or P-displacement controller. In this case, instead of feedback ω on the displacement, feedback on the displacement is required, which is best monitored by a pulse speed AM sensor. A pulse speed sensor, for example, one that emits 60 pulses per revolution, as well as digital controllers or displacement controllers, improve the accuracy of the control. To limit the starting currents of the AM during its intermittent movement, it is advisable to use a PI current controller, which is subordinated to a P-displacement controller.

The block diagram of a conveyor drive with a digital setpoint and a PI controller ω is similar to the diagram shown in Fig. 2. The circuit requires a DAT at the FC input and an ADT in the feedback loop for ω, if the sensor ω is a tachogenerator. Integration of the programmable setpoint and controller is acceptable by the method of rectangles or trapezoids. The same algorithms can be used for digital structural modeling of FC and AM. The integration time step can be taken during modeling to be the same for all links and less than 5-10 times the smallest time constant in the system. An 8- or 16-bit encoding of constant and variable parameters is acceptable. The following algorithms are recommended for the implementation and modeling of the functions of digital 3D and PI controllers ω.

For the setter:

$$U_{вих\,i} = U_{вих\,i-1} + (U_{вх\,i} - U_{вих\,i}/k_з) \cdot k_з \cdot H/T_{з\partial}), \qquad (15)$$

Where $U_{вх} = U_{Z0}$; $U_{вих} = U_Z$ (Fig. 2); H is the integration time step.

For the PI controller ω:

$$U_{вих\,1\,i} = U_{вих\,1(i-1)} + U_{вх\,i} \cdot H/T_{R1};$$
$$U_{вих\,i} = U_{вих\,1\,i} + U_{вх\,i} \cdot T_{R2}/T_{R1}, \qquad (16)$$

where $U_{вих1}$ is the intermediate value of the output voltage of the controller; $U_{вх} = U_Z - k_{ZN} \cdot N$; N is the speed of the AM ($N = \omega$).

The algorithms of the 3d and PI controller, as well as the I-link, which models the AM and the mechanism, are implemented in the form of subroutines function SAR3, function SAR4 and function SAR2 (see code below).

In this case, it is not necessary to model ADTs and DATs with transfer functions $W(s) = \frac{1 - e^{-(T_D \cdot s)/s}}{s}$, since the inputs of the AAS elements during the integration step H maintain the constant input values calculated in the previous step.

Typical microcomputers can be used for in-situ control of the drive and thermal energy sources, as well as other dryer equipment [7].

To evaluate the dynamic properties of the drive with a digital controller ω by the analytical method of constructing and analyzing lattice functions $h(iT_D)$, we present the following discrete transfer functions of the drive and the impulse H(z) function, where $z = e^{T_D \cdot s}$. These functions are obtained for the drive system, shown on Fig.2. For simplicity, the FC is assumed to be inertial-free and combined with the AM and DAT, and the inertial setpoint is not taken into account, since $h(iT_D)$ is calculated with a jump-like single signal 1(t) at the system input. Then the discrete transfer function of the open-loop drive system is equal to

$$W^p(z) = W_{peг}(z) \cdot Z\{W_{DAT}(s) \cdot W_{FC-AM}(s)\} =$$
$$= \left(k_R + \frac{z}{T_{R1}(z-1)}\right) \cdot Z\left\{\frac{1 - e^{-T_D \cdot s}}{s} \cdot \frac{k_\alpha \cdot k_{AM}}{T_м s + 1}\right\}, \qquad (17)$$

where T_D is the time of the period between discrete signals. After the transformations [1], we obtain

$$W^p(z) = k_c \cdot \frac{k_1 z - k_2}{k_3 z^2 - k_4 z + k_0}, \qquad (18)$$

where

$k_c = k_\alpha \cdot k_{AM} \cdot k_R$; $k_0 = e^{-T_D/T_м}$; $k_1 = (1 - k_0)(1 + 1/(k_R \cdot T_{R1}))$; $k_2 = 1 - k_0$; $k_3 = 1$; $k_4 = 1 + k_0$.

The discrete transfer function of the closed-loop drive system is as follows:

$$W^з(z) = \frac{W^p(z)}{1 + W^p(z) \cdot k_{ZN}} = \frac{b_1 z - b_0}{a_2 z^2 - a_1 z + a_0}, \qquad (19)$$

where $k_{ZN} = k_{з\omega}$;

$a_2 = 1$; $a_1 = k_4 - k_c \cdot k_1 \cdot k_{ZN}$; $a_0 = k_0 - k_c \cdot k_2 \cdot k_{ZN}$;

$b_1 = k_c \cdot k_1$; $b_0 = k_c \cdot k_2$.

The impulse $H(z)$ function is obtained as follows [1]:

$$H(z) = Z\{L[1(t)]\} \cdot W^з(z) = \frac{z}{z-1} \cdot W^з(z) =$$
$$= \frac{d_2 z^2 - d_1 z}{g_3 z^3 - g_2 z^2 - g_1 z - g_0}, \qquad (20)$$

where

$d_2 = b_1$; $d_1 = b_0$; $g_3 = a_2 = 1$; $g_2 = a_1 + a_2$; $g_1 = a_0 + a_1$; $g_0 = a_0$.

Determining the values of the coefficients d_i and g_j and dividing the numerator polynomial by the denominator polynomial, we obtain

$$H(z) = c_1 z^{-1} + \ldots + c_i z^{-i} + \ldots + c_n z^{-n}, \qquad (21)$$

where the coefficients c_i are the ordinates of and iT_D ($i = 1 \ldots n$) are discrete abscissa of the lattice function $h(iT_D)$.

The most complete assessment of the regulatory properties

of the actuator can be made by the time characteristics $\omega = f(t)$ and $M = f(t)$, obtained as a result of computer modeling of the actuator in the acceleration mode, and from experimental studies.

V. RESULTS OF CALCULATING THE PARAMETERS OF ELEMENTS AND MODELING THE CONVEYOR DRIVE

The main program and subroutines for digital structural modeling of the drive, based on the scheme shown in Fig. 2, are provided in the code below.

```
import numpy as np
def sign(x):
    if x > 0:
        return 1
    elif x < 0:
        return -1
    return 0
def SAR2(x, T1, H, y):
    return y + x * H / T1
def SAR3(x, T1, k, H, y):
    return y + (x - y / k) * k * H / T1
def SAR4(x, T1, T2, H, y1, y):
    y1 += x * H / T1, y = y1 + x * T2 / T1
    return y1, y
def SAR14(x, y0):
    return y0 * sign(x)
def SAR17(x, y0):
    y = x
    if abs(y) > y0:
        y = y0 * sign(y)
    return y
# Constants
L = 100 UZ0 = 10 KZ = 1 TZ = 0.01 TR1 = 0.01 TR2 = 0.04 UR0 = 12 KZN = 0.0665 KALP = 0.1 TTP = 0.005 UFN = 220 NO = 157 R1 = 8 R2 = 4.45 X1 = 5.2 X2 = 8 MO = 2 JS = 0.03 HI = 0.0001 D0 = 100 TMAX = 1
# Variables
UZ = 0 UR11 = 0 UR1 = 0 UR = 0 ALP = 0.05 SAD = 1 MOP = 0 T = 0 M = 0 N = 0 F = 0 D = 0
while T < TMAX:
    UZ = SAR3(UZ0, TZ, KZ, HI, UZ)
    UR11, UR1 = SAR4(UZ - KZN * N, TR1, TR2, HI, UR11, UR1)
    UR = SAR17(UR1, UR0), ALP = SAR3(UR, TTP, KALP, HI, ALP), F = R1 / ALP + R2 / (ALP * SAD)
    M = 3 * UFN**2 * R2 / (NO * ALP * SAD * (F**2 + (X1 + X2)**2)), SAD = 1 - N / (NO * ALP), MOP = SAR14(N, MO), N = SAR2(M - MOP, JS, HI, N), T += HI, D += 1
    if D >= D0:
        print(f'T: {T}, M: {M}, N: {N}')
        D = 0
```

The following drive parameters were used for modeling the conveyor system based on the FC-AM architecture with the selected AM type 4A80M4U3 and TP type TPTR-:6.3_400-200/50 UHL4. Motor: $P_н$ = 1.5 kW; $U_н$ = 380/220 V; $\omega_n = 150\ s^{-1}$; $\eta_n = 0.8$; $\cos\varphi_n = 0.87$; $J_д = 0.01\ kg\text{-}m^2$; $I_p/I_н = 6$; $M_P/I_н = 2$; $M_{kp}/I_н = 2.5$; I = 3.3 A; R_1 = 8 Ohm; x_1 = 5.2 Ohm; x_2 = 8 Ohm; $x_\mu = 1.9$; $s_n = 0.05$; $s_{cp} \approx 0.22$; $\omega_{cp} = 120\ c^{-1}$; $M_н$ = 10 nm; M_p = 20 nm; M_{cp} = 25 nm; M_{op} = 8 nm. Time constant of the mechanical T_M when moving on the working part of the characteristic ω = f (M) and f = 50 Hz - $T_M = J_\Sigma(\omega_0 - \omega_н)/M_н = 0{,}022\ s$, where $J_\Sigma \approx 3J_д = 0{,}03\ kg \cdot m^2$.

Equation of motion:

$$T_M \cdot d\omega/dt + \omega = \omega_0 - M_{on}(\omega_o - \omega_н)/M_н. \quad (21)$$

When moving on the start-brake segments of the characteristic $f = 50\ Hz$ $T_M = J_\Sigma \omega_{kp}/(M_{kp} - M_н) = 0{,}7\ s$ and the equation of motion:

$$T_M \cdot d\omega/dt - \omega = (M_n - M_{op})\omega_{kp}/(M_{kp} - M_{op}). \quad (22)$$

TP parameters: $k_{TP.U} = U_{фн}/U_{регн} = 220/10 = 22\ V/V$;

$k_{TPf} = f_н/U_{регн} = 50/10 = 5\ Hz/V$;

$f/U_ф = const$; $\alpha = f/f_н = U_ф/U_{Фн}$;

$k_{ALP} = \alpha_н/U_{регн} = 1/10 = 0{,}1$;

$T_{TP} = 0{,}005\ s$.

3D parameters ω: $k_z = 1$; $T_z < T_M \approx 0{,}1\ s$.

Parameters of the PI controller ω:

$T_{R1} = 2T_{TP} \cdot k_{ALP} \cdot k_{AD} \cdot k_{ZN} = 0{,}01\ s$,

where

$k_{AD} = \omega_н/\alpha_н = 150$; $k_{ZN} = U_{регн}/\omega_н = 0{,}0665\ V \cdot s$;

$T_{R2} \geq T_м$; .

while

$T_{R2} = 0{,}04\ s$; $k_R = T_{R2}/T_{R1} = 4\ V/V$; $U_{R0} = U_{R\max} = 12\ V$;

$N0 = \omega_{0f_н} = 157\ s^{-1}$; $M0 = 3\ nm$; $UFN = 220\ V$; and is the integration step: $HI = 0{,}001\ s$.

Acceleration simulation time: $T_{MAX} = 0{,}2\ s$; number of cycles in increments HI without outputting results $D0 = 2$.

The above data are used to model the drive on a computer. The time characteristics $\omega = f(t)$ and $M = f(t)$, obtained as a result of modeling the drive in the acceleration mode, are shown in Fig. 3. Their profiles differ from those of the natural acceleration characteristics of the asynchronous motor $\omega = f(M)$, because both the frequency f and voltage $U_ф$ are variable over time.

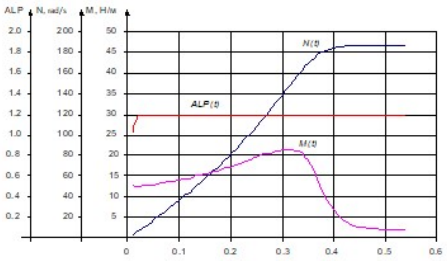

Figure 3. Dynamic characteristics of the drive by the FC-AM system during acceleration

VI. CONCLUSIONS

To improve the accuracy and coordinated control of medium temperature and conveyor movement with packages of printed products, as well as for controlling the motors of fans, dampers, and other dryer equipment, it is advisable to use a computer and a special software programs. It is advisable to adjust the power of heating lamps and the speed of the asynchronous drive of the conveyor with improved standard domestic thyristor converters, by replacing analog setpoints and regulators with software tools implementing the algorithms described in [8] and the current study.

The effectiveness of the developed digital automatic adjustment system (AAS) for controlling medium temperature and conveyor motion was confirmed through digital structural modeling. By applying the developed AAS on modern dryers, it is possible to experimentally study the dehydration processes of glued printed products and to determine the most appropriate, and eventually optimal, drying modes.

References

[1] Y. Chi, H. Xu, F. Sun, Y. Qian, *Hybrid Modeling Application in Control Valve*, Electrical Engineering and Systems Science, Systems and Control, 2020.

[2] L. Yan, Z. Duan, Q. Zhang, S. Niu, Y. Dong, C. Gerada. "Magnetic field and torque output of packaged hydraulic torque motor", *Energies*, vol.11, no. 1: 134, 2018. https://doi.org/10.3390/en11010134.

[3] N. Hanappier, E. Charkaluk, N. Triantafyllidis, "A coupled electromagnetic-thermomechanical approach for the modeling of electric motors," *Journal of the Mechanics and Physics of Solids*, vol. 10, p. 12-25, 2021. https://doi.org/10.1016/j.jmps.2021.104315.

[4] Y. Korkmaz, I. Topaloglu, H. Mamur, F. Korkmaz, "An investigation on switching behaviours of vector controlled induction motors", *Proceedings of the Third International Conference on Advanced Information Technologies & Applications*, Dubai, UAE, 7-8 November 2014, pp. 13-19. https://doi.org/10.5121/csit.2014.41102.

[5] F. Korkmaz, M. Çakır, İ. Topaloğlu, R. Gürbüz, "Artificial neural network based DTC driver for PMSM," *International Journal of Instrumentation and Control Systems (IJICS)*, vol. 3, no. 1, pp. 1-7, 2013. https://doi.org/10.5121/ijics.2013.3101.

[6] M. Farasat, M. N. Rostami, M. Feyzi, "Speed sensorless hybrid field oriented and direct torque control of induction motor drive for wide speed range applications," *Proceedings of the Power Electronic & Drive Systems & Technologies Conference, Teheran*, Iran, February 10-12, 2010, pp. 243–248. https://doi.org/10.1109/PEDSTC.2010.5471824.

[7] V. Bleizgys, A. Baskys and T. Lipinskis, "Induction motor voltage amplitude control technique based on the motor efficiency observation," *Electronics and Electrical Engineering*, vol. 3, pp. 68-72, 2011.

[8] O. Sytnikov, D. Skladany, S. Plashykhin, K. Sokolov, "Comparison of the efficiency of modern regulators in the spray dryer control system," *Bulletin of NTUU "Igor Sikorsky Kyiv Polytechnic Institute, Series: Chemical Engineering, Ecology and Resource Conservation*, no. 2, pp. 35-41, 2024. https://doi.org/10.20535/2617-9741.1.2024.300982. (in Ukrainian).

[9] I. Rehey, S. Ternytskyi, N. Kandiak, "Experimental analysis of corrugated fibreboard cutting with movable cutting disc during large-sized package manufacture," *Australian Journal of Mechanical Engineering*, vol. 20, issue 3, pp. 749-759, 2020. https://doi.org/10.1080/14484846.2020.1747734.

[10] L. Sikora, N. Lysa, O. Fedevych, B. Fedyna, "Information technology of thermodynamic interaction of laser radiation quality upgrade while drying book blocks," *International Journal of Computing*, vol. 23, issue 4, pp. 592-597, 2024. https://doi.org/10.47839/ijc.23.4.3758.

[11] K.N. Kotsoglou, A. Biedermann "Polygraph-based deception detection and machine learning. Combining the Worst of Both Worlds?", *Forensic science international. Synergy*, 9, 2024. https://doi.org/10.1016/j.fsisyn.2024.100479.

[12] K. A. Smith, *Non-Adhesive Binding*, Vol. 4: Smith's Sewing Single Sheets, Paperback, New York, USA, 2001, 336 p.

[13] O. Alves-Filho "Energy effective and green drying technologies with industrial applications", *Chemical Engineering Transactions, AIDIC-Italian Association of Chemical Engineering*, vol. 70, pp. 145-150, 2018.

[14] J.Sousa, L. Figueiredo, C. Ventura, J.P. Mendonça, J. Machado, "Development of an innovative mechatronic binder machine", *Sensors*, 22(3), 741, 2022. https://doi.org/10.3390/s22030741.

[15] R. Bradbury, "Thermal printing", *Chemistry and Technology of Printing and Imaging Systems*, pp. 139-167, 1996. https://doi.org/10.1007/978-94-011-0601-6_6.

[16] C. Guo, S.C. Singh *Handbook of Laser Technology and Applications: Laser Design and Laser Systems (Volume Two)*, 2nd ed., CRC Press, Boca Raton, Florida, USA, 2021, 716 p. https://doi.org/10.1201/9781315310855.

[17] K. An, *Fundamentals of Laser Physics*, WSPC, Singapore, 2023, 322 p.

[18] Z. Shen, D. Guo, H. Zhao, W. Xia, H. H. Wang, *Laser self-mixing interferometer for three-dimensional dynamic displacement sensing*, *IEEE Photonics Technology Letters*, vol. 33, issue 7, pp. 331-334, 2021. https://doi.org/10.1109/LPT.2021.3062287.

[19] P. Lutzmann, R. Frank, M. Hebel and R. Ebert, "Potential of remote laser vibration sensing for military applications," *Proceedings of the OPTRO 2005 Symposium*, Paris, vol. 37, pp.1-12, 2005.

[20] G. Caprara, D. Cervone, *Personality: Determinants, Dynamics, and Potentials*, Cambridge University Press, UK, 2000, 506 p. https://doi.org/10.1017/CBO9780511812767

[21] R. Farnood, "Review: Optical properties of paper: theory and practice", *Advances in Pulp and Paper Research*, Oxford 2009, Trans. of the XIVth Fund. Res. Symp. Oxford, 2009, pp 273–352, FRC, Manchester, 2018. https://doi.org/10.15376/frc.2009.1.273.

[22] G. Soares, C. Modarres, M. Kaminskiy, M. Krivtsov, *Reliability engineering and risk analysis: a practical guide*, Elsevier, Amsterdam, Netherlands, 1999, 542 p.

[23] C. Florian, P. Serra, "Printing via laser-induced forward transfer and the future of digital manufacturing", *Materials*, 16(2): 698, 2023. https://doi.org/10.3390/ma16020698.

[24] Z. He, K. Zhang, B. Wei, J. Huang, Y. Wang, E. Li, "Path tracking control of high-speed intelligent vehicles considering model mismatch", *International Journal of Robust Nonlinear Control*, 35(1), pp.168-187, 2025. https://doi.org/10.1002/rnc.7640.

[25] J.R. Howell, M.P. Menguc, R. Siegel, *Thermal Radiation Heat Transfer (6th ed.)*. CRC Press, USA, 2015, 1016 p. https://doi.org/10.1201/b18835.

***Bohdana Fedyna** received the philosophy of doctorate degree in Information Technologies from Ukrainian Academy of Printing in 2017. She is currently working as an Associate Professor at the Department of Computer Technologies in Publishing and Printing Processes, Lviv Polytechnic National University. Her research areas include design of hardware and software tools for the automation of printing production processes.*

***Olga Fedevych** received the philosophy of doctorate degree in Information Technologies from Lviv Polytechnic National University in 2018. Currently working as an Associate Professor at the Department of Automated Control Systems, Lviv Polytechnic National University. Her research areas include web cyber security, trends forecasting, and process modelling analysis. She has been serving as a reviewer for many journals.*

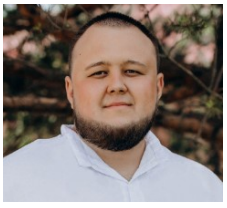

***Yurii Lysyi** graduated from the Department of Automation of the Ukrainian Academy of Printing with a master diploma with honors. Currently working as Postgraduate student of the Institute of Printing and Media Technologies, Department of Computer Technologies in Publishing and Printing Processes, Lviv Polytechnic National University. His research areas include information technologies in printing, software tools design, and media technologies.*

***Natalia Lysa** received the philosophy of doctorate degree in Information Technologies from Lviv Academy of Printing in 2012, and her Doctor of Technical Sciences from Lviv Academy of Printing in 2019 respectively. Currently working as an Associate Professor at the Department of Automated Control Systems, Lviv Polytechnic National*

University. Her research areas include process modelling analysis, information and telecommunication management technologies, information technologies in ecology and medicine.

***Liubomyr Sikora** received the Doctor of Technical Sciences from Ukraine Academy of Sciences State Research Institute of Information Infrastructure in 2001. He is currently working as a Full Professor at the Department of Automated Control Systems, Lviv Poly-technic National University. His research areas include integrated hierarchical control systems, digital signal processing, information technologies in complex systems.*